Review

polymers advanced technologies

Received: 4 June 2012, Accepted: 5 June 2012, Published online in Wiley Online Library

(wileyonlinelibrary.com) DOI: 10.1002/pat.3054

Conjugated polymers - carbon nanotubes-based functional materials for organic photovoltaics: a critical review

Céline Bounioux[a], Eugene A. Katz[a,b] and Rachel Yerushalmi – Rozen[b,c]*

Conjugated polymers and carbon nanotubes (CNTs) are important constituents of modern functional hybrid materials. Their utilization as photoactive layers in organic solar cells requires better understanding of the relation between the structure and composition of the hybrids and their photovoltaic efficiency. While fullerenes-conjugated polymer hybrids have been intensively studied over the last two decades, far less is known about the linkage between processing conditions, interfacial interactions, self-assembled structures and functionality in CNT-conjugated polymers composites. This article reviews some of the studies carried over the last decade and highlights the challenges in both fundamental understanding and technological manipulation of these materials. Copyright © 2012 John Wiley & Sons, Ltd.

INTRODUCTION

Conjugated polymers are functional materials that lie at the heart of organic photovoltaic devices used to convert light into electricity. With a theoretical limit of power conversion efficiency (PCE) around 23%,[1] polymer-based organic photovoltaics (POPV) have the potential for creating a steady, sustainable, industrial technology based on environmentally benign materials with almost unlimited availability. Due to their high processability at relatively low temperatures, mostly from solutions, conjugated polymers are a less expensive alternative to inorganic semiconductors fabricated from silicon, gallium and arsenic, etc. Light, flexible, large area panels can be produced using high throughput low-cost role-to-role printing processes.[2,3] "Plastic" solar cells are expected to offset costs and draw a shorter energy pay-back of investment over time as compared to silicon-based solar cells and create a new market of low-priced electronics, once two essential challenges are resolved: These are the low PCE (efficiency) and short life-time of POPV devices under operational conditions. Currently, the record PCE for POPV, which is defined as the percentage of maximum electrical power generated by a solar cell with respect to the power of the incident light, is above 8%[4] while that of crystalline silicon is 25%.[5] The operational lifetime of POPV cells previously measured in minutes can now, in favorable circumstances, exceed many thousands of hours.[6] These improvements have been achieved via continuous scientific and technological efforts over the last ten years.

A major breakthrough in the utilization of conjugated polymers as materials for POPV came with the development of hybrid structures containing conjugated polymers and carbonaceous electron accepting nanostructures (fullerenes and fullerene derivatives), following the discovery of the photoinduced electron transfer between poly(para-phenylenevinylene) (PPV) derivative poly[2-methoxy-5-(2-ethylhexyloxy)-1,4-phenylenevinylene] MEH-PPV and the C_{60} Buckminsterfullerene.[7,8]

Carbon nanotubes (CNTs) were first introduced into POPV as a bi-layer comprising PPV-CNT in 1999, by Ago *et al.*[9] In years to follow, PV-active CNT-conjugated polymers hybrids have aroused considerable interest. Initially, CNTs were presented as candidates for replacing fullerenes as electron acceptors. The measured efficiency of hybrid CNT-conjugated polymer solar cells turned out to be extremely low (below 0.1%),[10] and only recently dramatic improvement was obtained reaching 4.1% in boron-doped CNT.[11] Nowadays, it seems that CNTs may function in a variety of different roles: semiconducting CNTs (s-CNTs) are expected to be directly active in charge separation, while both metallic and s-CNTs should enhance charge collection and charge transport, and indirectly improve the crystallization of the conjugated polymer. Each of these is expected to contribute to PCE improvement in CNT-based POPV.

In this article, we briefly describe the major players; conjugated polymers, fullerenes and CNTs, and highlight their role in POPV. We then outline the evolution of conjugated polymers-CNT hybrids as functional materials for OPV applications emphasizing the linkage between the physical interactions at the conjugated polymers-CNT interface and the photovoltaic performance of the resulting hybrids.

CONJUGATED POLYMERS IN POPV

Conjugated polymers-based electronics has emerged from the discovery in the 1970s by Shirakawa, MacDiarmid and Heeger[12]

* *Correspondence to: Rachel Yerushalmi – Rozen, Dept. of Chemical Eng., Ben-Gurion University of the Negev, Beer-Sheva 84105, Israel. E-mail: rachely@bgu.ac.il*

a *C. Bounioux, E. A. Katz*
Dept. of Solar Energy and Environmental Physics, Jacob Blaustein Institutes for Desert Research, Ben-Gurion University of the Negev, SedeBoker campus, 84990, Israel

b *E. A. Katz, R. Yerushalmi – Rozen*
Ilze Kats Institute for Nanoscale Science and Technology, Ben-Gurion University of the Negev, Beer-Sheva 84105, Israel

c *R. Yerushalmi – Rozen*
Dept. of Chemical Eng., Ben-Gurion University of the Negev, Beer-Sheva 84105, Israel

that the conductivity of polyacetylene (CH)x films could be increased by several orders of magnitude via oxidation (p-doping) of the polymer backbone.

A conjugated polymer comprises an alternating single and double carbon–carbon bonds. Single bonds are known as σ-bonds and are associated with localized electrons, and double bonds comprise both a σ-bond and a π-bond. The π-electrons are more mobile than the σ-electrons and are delocalized due to the mutual overlap of π-orbitals along the conjugation path, which causes delocalization of the wave functions over the conjugated backbone.[13]

The π-bands are either empty, where the lowest orbital is referred to as that lowest unoccupied molecular orbital (LUMO), or filled with electrons, where the highest orbital is referred to as the highest occupied molecular orbital (HOMO). The bandgap (difference between HOMO and LUMO) of conjugated polymers ranges from 1 to 4 eV.[14]

The electrical and optical properties of conjugated polymers may be readily tailored via organic synthesis enabling enhancement of the inherently high optical absorption coefficient (~10^5 cm^{-1}) and consequentially utilization of thin (100–200 nm) films as the active layers in solar cells.[14]

However, high absorption is not enough, and materials that are designed to function as advanced POPV materials should exhibit also suitable location of the HOMO–LUMO levels, solubility in common organic solvents, ability to easily form films on a variety of substrates when applied via common techniques such as spin-casting or dip-coating, partial miscibility with common electron acceptors (such as fullerenes), high hole mobility in the solid state (whether amorphous or semi-crystalline), and some degree of chemical stability in ambient conditions. It is clear that only few polymers can meet the long list of requirements presented above. In addition, as some of the requirements are inherently contradictory, optimization is necessary. Surprisingly, over the years, a few classes of conjugated polymers were developed and utilized successfully in POPV applications.[13,14]

Initially two of the most common classes of useful polymers were derivatives of poly(phenylene-vinylene), (PPV) and polythiophenes. As PPV and polythiophenes are practically insoluble, alkyl or alkoxy chains were covalently linked to the phenylene rings as in poly[[(2-ethylhexyl)oxy]methoxy-1,4-phenylene]-1,2-ethenediyl], MEH-PPV to make the material soluble in common organic solvents such as chloroform, chlorobenzene and toluene. As for the polythiophenes, alkyl side chains (C_nH_{2n+1}) are introduced in the 3- position[12] so as to improve the solubility of the original polythiphenes.

Poly(phenylenevinylenes)

PPV and PPV (Fig. 1(a)) derivatives have been synthesized using numerous procedures (for a review, see ref.[15]). The major absorption band of PPVs is in the range of 400–500 nm with a bandgap of 2.1–2.7 eV.

Poly(thiophenes)

Polythiophenes display a unique combination of efficient electronic conjugation, synthetic versatility and chemical stability. Two of the polythiophenes deserve special attention: Regio-regular poly(3-hexylthiopehene) rr-P3HT (Fig. 1(b)), which is the best performing derivative of the poly(3-alkyl thiophene) P3ATs family, and poly(3,4-ethylenedioxythiophene), PEDOT (Fig. 1(c)), which is an important organic conductor used in a large variety of applications.

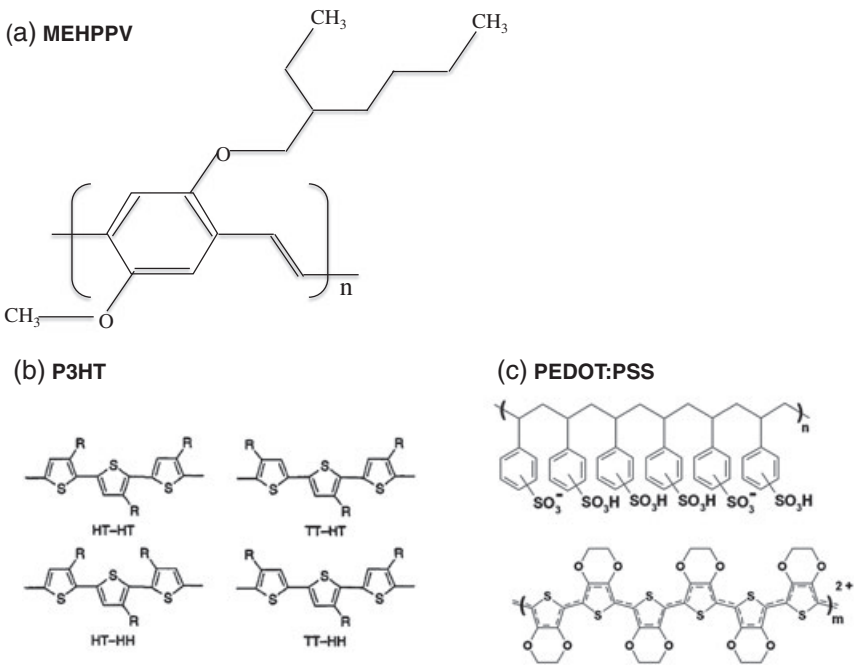

Figure 1. Schematic structures of polymers used in POPV (a) MEHPPV. (b) The four possible triads resulting from attachment of hexyl side chains to the three-position of the thiophene rings (adapted from ref. 18). The stereoregular head-to-tail (HT) configuration is preferred over the head-to-head (HH) or tail-to-tail (TT) configurations. GRIM and Reike method[17] allow for the synthesis of P3HT with a high degree of regioregularity which denotes the percentage of HT configuration that may be as high as 99% in P3HT. High molecular weight (Mn) and relatively narrow polydispersity index (PDI) (1.1–1.3) with specific end-groups may also be obtained. (c) A water solvated PEDOT:PSS complex.

P3ATs are comb-like polymers where the main chain is composed of covalently linked thiophene rings. rr-P3HT with almost exclusive head-to-tail geometry (Fig. 1 (b)) can be prepared via two well-established routes, the Grignard Metathesis method, pioneered by McCullough and coworkers,[16] and the Reike method.[17]

The regiorandom material absorbs at around 425 nm, while the absorption of the regioregular material is red-shifted to 450 nm. Also, the emission spectra differ with a maximum of 570 nm for the rr-P3HT and 550 nm for the random P3HT.

Another popular derivative is poly(3-octylthiophene) P3OT. Due to the longer alkyl chain, P3OT of similar molecular weight as P3HT is more soluble and thus easier to processes while the typical degree of crystallinity of P3OT is lower and the optical behavior is somewhat modified.[18]

PEDOT[19] is synthesized from the EDOT monomer using standard oxidative chemical or electrochemical polymerization methods to yield insoluble oligomers (of up to about 20 repeat units) that are unstable in the neutral state. It was found that it is possible to solubilize the PEDOT by addition (during polymerization) of poly (styrene sulfonic acid), or the sodium salt, (PSS) as a charge-balancing dopant. The formation of PEDOT:PSS complexes as presented in Fig. 1(c) yields dispersions that can be easily processed to form thin films of high conductivity (ca. 10 S/cm), high visible light transmissivity and excellent stability.[19] Aqueous dispersions of PEDOT:PSS of different PEDOT to PSS ratios, surface tension and pH are commercially available. Thin films of PEDOT:PSS are being used in applications where transparent conductive layers are required, such as hole-transporting electrode coating in POPV, antistatic coatings and electronic paper. The conductivity of PEDOT:PSS layers is sensitive to the conformational state of the polymeric complex, the abundance of benzoid versus quinoid states of the EDOT units, and the assembly of the molecular moieties in the dispersion.[20]

Band-gap tuning

The majority of commercially available semiconducting polymers have high bandgaps around 2.0 eV (600 nm). This limits the absorption of POPV to below 30% of the solar spectrum as the solar emission peaks around 1.77 eV. Low bandgap with E_g of ~1.2–1.8 eV (1000 nm) enables absorption of 85% of the solar radiation on earth.[21]

Several structural factors influence the bandgap of a conjugated polymer; bond length alteration of the ground state conformations, aromaticity and substituents. The effect of each of these parameters on the properties of conjugated polymers has been discussed comprehensively by Winder and Sariciftci.[22] In general, the bandgap may be lowered by increasing the conjugation length. Thus, structural modifications that decrease the conjugation length such as incorporation of aromatic units that confine the π-electrons, and induction of torisonal strain that reduces the overlap of the π-electrons are to be avoided. The energy bandgap may also be modified via the interplay between electron donating and electron accepting groups. Thus, low band-gap polymers may be based on fused ring systems (for example poly(isothianaphthene, PITN, with $E_g = 1.0$ eV[23]) or copolymers with alternating donor and acceptor groups (for example benzothiadiazole and thiophene, BPT).[24]

Condensation polymerization of 2,5-bis(5-trimethylstannyl-2-thienyl)-*N*-dodecylpyrrole and 4,7-dibromo-2,1,3-benzothiadiazole enables the preparation of a conjugated oligomeric material (PTPTB), with an optical bandgap of $E_g = 1.60$ eV, as a result of the alternation of electron-rich and electron-deficient units along the chain.[25,26]

Another example for a low band-gap polymer with $E_g = 1.46$ eV is poly[2,6-(4,4-bis- (2-ethylhexyl)-4 *H*-cyclopenta[2,1-b;3,4-b]-dithiophene)-*alt*-4,7-(2,1,3-benzothiadiazole)] (PCPDTBT). Fused ring systems, such as those presented in Fig. 2(a), enhance the quinoid resonance structure, which in turn reduces bond alteration.[27]

Recently, it was demonstrated that it is possible to design and prepare a series of low band-gap block-copolymers exhibiting bandgaps of 1.77 to 1.24 eV in the solid state, absorption at the optimal wavelengths and processability from solution:[28] Diketopyrrolopyrrole (DPP) was covalently linked to electron-rich aromatic segments to form a series of low band-gap alternating copolymers: 3,6- bis(5-bromo-2-thienyl)-2,5-dihydro-2,5-dialkyl-pyrrolo[3,4-c]pyrrole- 1,4-dione (DPP2T) with 9,9-dioctylfluorene (F) and 4,4-dioctylcyclopenta[2,1-b:3,4-b0]dithiophene (CPDT) using Suzuki coupling.

While improved solar light harvesting is achievable in low-band-gap polymers, charge separation efficiency and transport of free charge carriers to the relevant electrodes depend mainly on the phase morphology of the conjugated-polymer fullerene (acceptor) hybrids which is determined by the physical interactions between the polymer molecules and the electron accepting phase (fullerenes).

Doping and chemical stability

Doping of π-conjugated systems can increase the conductivity by 10 orders of magnitude transforming the polymers from insulators to conductors.[29] Both n-type (electron donating) and p-type (electron accepting) doping have been demonstrated. In conjugated polymers, the dopants are positioned interstitially, between the chains, and exchange charges with the polymer backbone. The counter ions that are not covalently bound to the polymer, but are held by electrostatic forces, are known to distort the bond length of the intra-chain bonds. π-conjugated polymers are inherently sensitive to the presence of both oxygen and water due to their relatively low redox potential. Stability to ambient conditions requires an ionization potential that is higher than 4.9 eV.[30] When lower, spontaneous oxidation will lead to formation of charge-transfer complexes between the thiphene molecules and oxygen under illumination. The complex promotes the formation of a singlet oxygen which reacts with the polymer leading to irreversible chemical degradation.[30] A thorough discussion of stability is beyond the scope of this review and will only be mentioned intermittently.

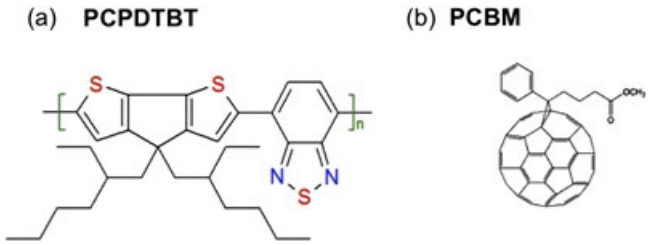

Figure 2. (a) Poly[2,1,3-benzothiadiazole-4,7-diyl[4,4-bis(2-ethylhexyl)-4 H-cyclopenta[2,1-b:3,4-b']dithiophene-2,6-diyl, PCPDTBT (b) [6]-phenyl C_{61} butiryc acid methyl ester, PCBM. This figure is available in colour online at wileyonlinelibrary.com/journal/pat

FULLERENES AND FULLERENES DERIVATIVES

Fullerenes are fully conjugated, all-carbon closed-cage molecules in the form of convex polyhedra containing only hexagonal and pentagonal faces (C_{20}, C_{24}, C_{26}... C_{60}... C_{70}, C_{72}, C_{74}...). The most abundant and stable member of the family is C_{60}, shaped as a soccer-ball truncated icosahedron.[31] Theoretical predictions indicate that the LUMO of C_{60} is energetically low lying and triply degenerate, and capable of accepting at least six electrons upon reduction.[32] Experimental measurements have shown that that C_{60} is fully conjugated.[32–34] The 12 pentagons in C_{60} arrange in the form of six pyracylene units and are connected to each other via 30 bent π-bonds. Addition of one electron to each pyracylene unit creates aromaticity in one of the pentagonal rings. While electron capture increases the sp^3 character of the molecule and reduces the strain energy, electron loss increases the sp^2 character and the ring strain. Hence, the electron affinity and ionization potential of C_{60} are high, and electrochemical reduction of C_{60} up to the -6 state can be accomplished.[32]

One of the most common chemically functionalized fullerenes is methanofullerene, [6,6]-phenyl C_{61} butiryc acid methyl ester, PCBM (Fig. 2 (b)). A short aliphatic chain (six carbons) with hydrophilic group at its end provides PCBM with improved solubility in organic solvents. PCBM is used as an electron acceptor in the active layers of molecular electronics and in particular in rr-P3HT-based POPV, allowing efficient exciton dissociation at the PCBM-polymer interface. The latter results from the good matching in the energy levels between P3HT and PCBM.

POLYMERIC SOLAR CELL

PV solar cells convert solar energy to electrical power: following the absorption of a photon, an electron may be excited to a higher energy level. If a conventional *inorganic* semiconductor solar cell is illuminated by photons of energy higher than the bandgap E_g of the semiconductor, pairs of electrons and holes are generated. The photoinduced charge carriers then migrate to a junction between two materials across which there is an electrochemical potential difference in equilibrium (usually, this is a p-n junction, formed between p- and n-doped semiconductor).[14] Figure 3 summarizes the parameters used to characterize solar cells.

In POPV, the photovoltaic processes are initiated by photon absorption by the conjugated polymer, formation of a bound electron–hole pair known as an *exciton*, exciton diffusion followed by separation into free charge carriers at the polymer–fullerene interface and charge collection by the electrodes. The cell current Isc is determined by the number of free charge carriers that finally reach the electrodes. Being multiplied by open-circuit voltage (V_{oc}) and fill factor (FF), this quantity defines the POPV efficiency (the terms are defined in Fig. 3).

The essential difference between POPV and inorganic solar cells is the primary photoexcitation step: In organic materials, absorption of light does not lead to the formation of free charge carriers but to the formation of coulombically bound electron–hole pairs, the excitons. The nature of these neutral excited states in conjugated polymers has been discussed at length over the last years.[35] In particular, the actual value of the electron

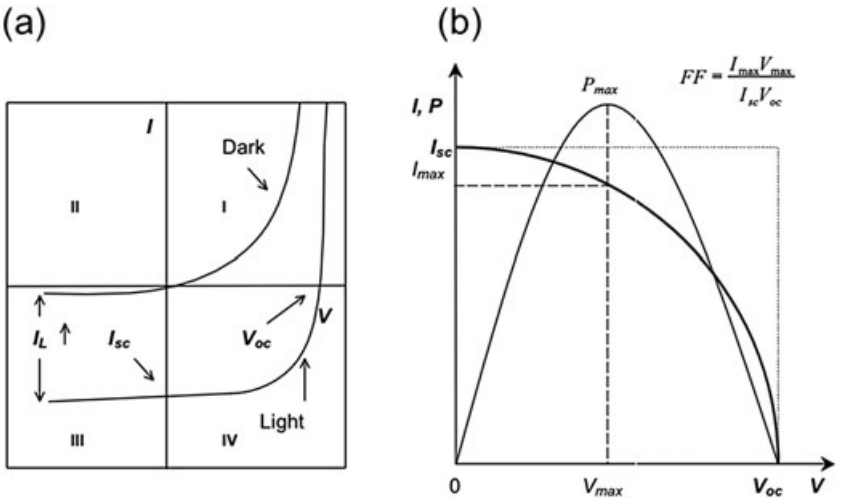

Figure 3. Solar cells parameters (a) current–voltage (I–V) curves without illumination (dark) and with illumination (light) are represented on a I–V diagram. The parameters that define the performance of a solar cell are the short-circuit current, I_{sc}, and the V_{oc}. (b) Here, the I–V curve (light) of the fourth quadrant is displayed after inversion around the voltage axis. Power (P = I·V)–voltage curve is shown as well. The maximum power, P_{max}, I_{max} and V_{max}, corresponding to the current and voltage, respectively, at maximum power output $P_{max} = I_{max} \times V_{max}$ are also defined in this part of the figure. Solar cell parameters such as the I_{sc}, V_{oc}, FF and the power conversion efficiency (PCE), η, are defined below: For $V = 0$, $I = I_{sc}$, and for $I = 0$, $V = V_{oc}$ the FF is

$$FF = \frac{I_{\max} \times V_{\max}}{V_{oc} \times I_{sc}}$$

and the PCE or h is defined as:

$$\eta = \frac{I_{\max} \times V_{\max}}{P_{in}} = FF\frac{V_{oc} \times I_{sc}}{P_{in}}$$

where P_{in} is the power of the incident light.

and hole binding energy has been a matter of intense debate (anyway, it is of order of 100 meV compared to a few meV for an inorganic semiconductor).[36] The binding energy of excitons in POPV is a manifestation of weak (intermolecular) interactions among the molecules and the consequential low dielectric constant (typically 2–4) that characterizes organic materials.[14,21]

Excitons may either recombine, and the absorbed photons will be wasted or they may diffuse in the active layer until they arrive at a dissociation site, a potential step formed at the interface between an electron donor and an electron acceptor in the active layer (energy diagram describing the process is shown in Fig. 4(a)). As the diffusion length of excitons is in the range of 3 to 10 nm in polymers,[37] only dissociation sites located within this distance are relevant for splitting of the neutral excitons into charge carriers.

Following exciton splitting, the free charge carriers further drift to the device's respective electrodes via two separate channels, holes via the conjugated polymer phase (to the anode) and electrons via the fullerene or fullerene-like phase (to the cathode), thus providing the current that is injected to the external circuit.

V_{oc} in POPV is controlled mostly by the chemical potential energy gradient created by exciton dissociation (charge transfer). Understanding of the physical origin of the V_{oc} is critical for performance improvement of solar cells. While well understood for inorganic PV, it is still a matter of debate for the POPV devices. It has been accepted, however, that the upper V_{oc} limit depends on the effective heterojunction energy gap (Fig. 4(a)), that is the difference between the LUMO level of the n-type (acceptor) material and the HOMO level of the p-type (donor) moiety of the active layer, E_g = LUMO(A)-HOMO(D).

Initially, polymer-based solar cell were designed as a double layer of polymer donor and acceptor between two electrodes (Fig. 5 (a)), while currently mostly bulk heterojunction (BHJ) architecture is used (Fig. 5(b)).[38] The BHJ architecture was engineered

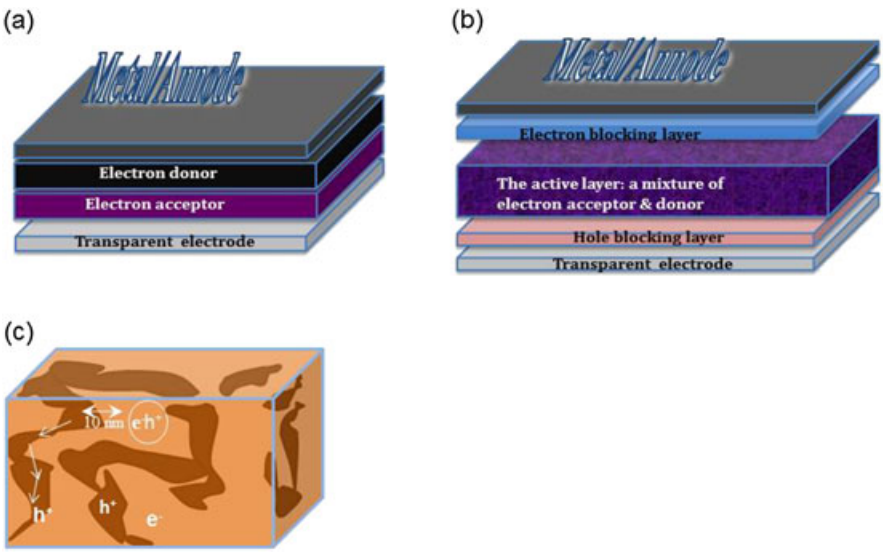

Figure 4. An illustration of (a) a double layer POPV and (b) BHJ device architectures (c) The mesoscopic structure of the active layer. The different colors represent fullerene-rich (bright) and polymer-rich (dark) regions. This figure is available in colour online at wileyonlinelibrary.com/journal/pat

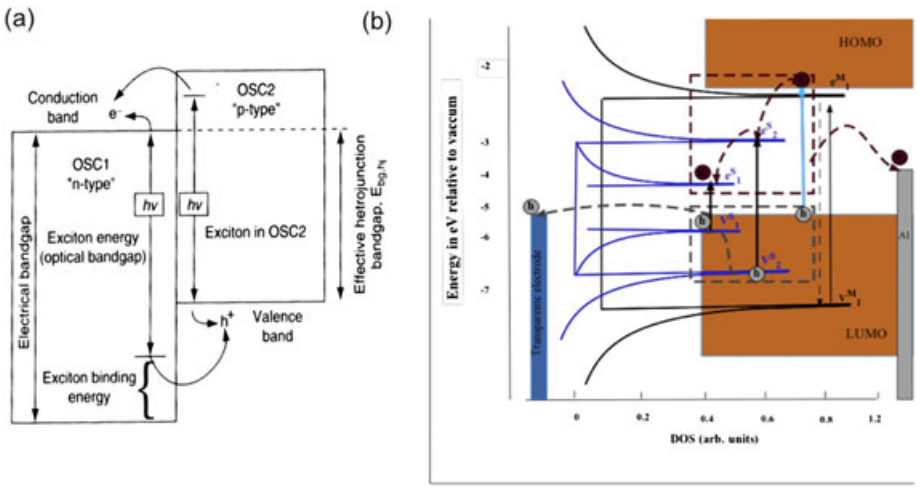

Figure 5. (a) Energy diagram for charge transfer and V_{oc} formation at the interface between p-type (donor) and n-type (acceptor) parts of the POPV photoactive layer. (b) Schematic energy diagram of the photo excitation processes in a POPV cell comprised of MEH-PVV/SWCNT photoactive layer, ITO and Al electrodes. Optically allowed electronic transitions are indicated with vertical arrows, whereas dashed arrows indicate nonradiative paths (following Kazaoui, S., *et al.*, ref. 44). This figure is available in colour online at wileyonlinelibrary.com/journal/pat

so as to optimize both charge separation and charge carriers transport.[38] Thus, the BHJ structure offers a structural compromise between two seemingly contradicting morphological requirements: multiplicity of small domains with maximal surface area that are separated by typical distances of 10 nm and continuous (percolated) pathways for holes (in the donor channel) and electrons (in the acceptor channel)) in both polymer and the fullerenes phases, respectively (Fig. 5(c)).When first introduced, BHJ type cells have considerably increased the power conversation efficiency of POPV to above 1%.[38] Today, this is the most popular configuration in conjugated polymers-based solar cells with PCE of above 8%.[4]

Charge transport in conjugated polymers is highly non-isotropic: *Intramolecular* charge transport along the polymer backbone is much more efficient than *intermolecular* transport across the polymer chain. In the second case, the mechanism is called the "hopping" process.[38]

Hopping is also the mechanism responsible for electron transport between the fullerene molecules in the fullerene channel.[39] That, along with the spherical geometry of the fullerenes, and the phase diagram of the combined system result in the need to use high fullerene concentrations. For example, 67 wt% PCBM is used with poly(2-methoxyl-5-(3,7- dimethyloctyloxy)-para-phenylene-vinylene] (MDMO-PPV).[40] As these carbonaceous moieties absorb mainly in the UV, harvesting of the solar energy is far from optimal. The relatively high fraction of the fullerene derivatives was also found to limit the crytallinity of the (semi-crystalline) polymer phase leading to to deterioration of charge (hole) mobility in the polymeric matrix and also reduction of the mechanical properties of the layer, as compared to those of the pristine polymeric layer.

CARBON NANOTUBES

In the quest for improved performance, CNT were suggested about a decade ago as an efficient alternative to fullerenes and fullerene derivatives. CNT are cylindrical tubes of graphene. Single-walled CNTs (SWCNTs) comprise a single graphene layer, and they are either metallic or semiconducting depending on their chirality.[41] Multi-walled nanotubes (MWCNTs) (Fig. 6 (a), (b)) are composed of 2–100 layers of nested graphene cylinders with an interlayer spacing of 0.34–0.36 nm, similar to the typical spacing of turbostratic graphite, and they are metallic. The typical diameter of a SWNT is 0.4–3 nm and 1.4–100 nm for MWNT. The length of a tube can reach millimeters, and thus the aspect ratio (length to diameter ratio) of CNT may be higher than 1,000,000[42] leading to the formation of percolated networks in a medium at concentrations below 0.1 wt%.[43] SWCNT combine superior electron transport properties with reduced charge carrier scattering (room temperature ballistic transport) offering a high-mobility pathway for charge carriers transport. The latter enables them to carry large currents with essentially no heating of an estimated current density of 10^9 A/cm^2 (compared to that of copper, 10^6 A/cm^2)[44] and carrier mobility of (~100,000 cm^{2}Vs).[44]

The energy bandgap, E_g, in semiconducting nanotubes (s-SWCNT) is inversely related to the diameter of the tube and ranges from 0.48 to 1.37 eV. Depending on their E_g, CNT absorb light (mostly in the IR). They are expected to act as electron acceptors under the appropriate conditions. CNT also exhibit superior mechanical properties.[41]

For efficient charge separation, the LUMO of the donor material (conjugated polymer) should be located sufficiently above

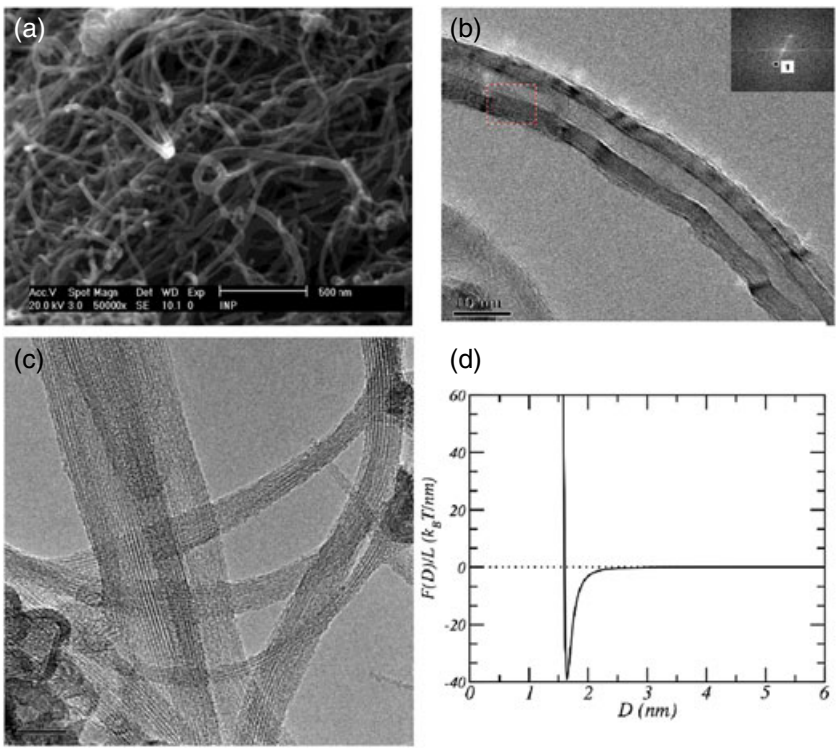

Figure 6. (a) A high-resolution SEM image of as-synthesized powder of MWNT (INP, Toulouse, France). (b) HRTEM image of an individual MWNT (Arkema, France C100). FFT of the diffraction image reveals that the distance between plains about 0.364 nm. (c) A HRTEM image of a SWNT bundle (NanoCarbLab (NCL) Russia. (d) Interaction potential between two parallel SWNT in vacuum, as a function of the distance between them, as derived from the Girifalco potential.[57] Note the very deep attractive well when the SWNTs are at contact and the contact energy of 40 k_bT per nm.[58] This figure is available in colour online at wileyonlinelibrary.com/journal/pat

the LUMO of the acceptor (CNT), and the HOMO level of the acceptor should be below the HOMO of the donor, with potential difference that exceeds the exciton's binding energy.[45] While such band offsets occur at the interface between C_{60} (or its derivatives) and most commercially available conjugated polymers, the dependence of CNT energy levels on their diameter and type results in heterogeneity in their electronic behavior and is one of the hurdles for their utilization in POPV.

In Fig. 4(b), we present a schematic energy diagram of a conjugated polymer-CNT device. While it can be seen from the diagram that some types of SWCNT carry a potential to serve as electron acceptors, their actual behavior is still questionable. Several studies aimed to investigate photoinduced charge transfer in CNT-polymer systems. Most of them utilized indirect methods such as quenching of the polymer photoluminescence or a faster decay of the emission as indications for electron transfer. Careful examination of the literature reveals that only a few studies have reported what may be considered an unambiguous evidence of photoinduced electron transfer between conjugated polymers and SWCNT.

The first solid evidence for charge transfer between SWCNTs and conjugated polymers (MEH-PPV) was provided by Yang *et al.* in 2003[46] using photoinduced absorption spectroscopy. In their study, photoinduced charge transfer was deduced from the observed reduction of the emission from the polymer and an increase of the polaron peak in the MEH-PPV-SWCNT hybrids. Comparison with a C_{60}-MEHPPV blend indicated that electron transfer was less efficient in the CNT-polymer blend than in the polymer-fullerenes blend. The authors suggested that the origin of these phenomena is the lower electron affinity of the SWCNT as compared to the fullerenes. However, one cannot exclude the suggestion that poor dispersion of the SWCNT within the polymer and the low purity of the CNT sample may have been the reason for the inefficient electron transfer measured in the experiments.

Calculations by Luo *et al.*[47] suggested that SWCNT have a higher electron affinity than C_{60} and its derivatives. Yet, experimental measurements of the conductance of SWCNT indicated that the tubes behave as p-type semiconductor (rather than n-type expected for electron acceptors). This behavior was attributed to experimental artifacts or chemical modification of the tubes probably due to adsorbed oxygen.[48]

Recently, it was shown via a combination of steady-state and time-resolved spectroscopy that the excited state of P3HT is quenched in the presence of SWCNT.[49] The study demonstrated charge transfer (in addition to previously observed energy transfer) leading to the formation of long-lived charge carriers. Light-induced electron spin-resonance ([50,51]) was used as well to probe the primary stage of photogeneration of unbound electron and hole due to charge transfer. Yet, the interpretation of the results suffered from the structural heterogeneity of powder-synthesized CNT and the consequential variability of their electronic (as well as optical) properties.

Engineering of CNT-based photo-active hybrids

The inherent properties of CNT presented so far suggest that these nanostructures should provide a ballistic transport route for electrons already at minute CNT concentrations providing an alternative to the inefficient electron transport mechanism (hopping) of the fullerenes. Furthermore, some of the s-SWNTs may act also as efficient electron acceptors when mixed with the "work-horse" of the field, rr-P3HT[21] due to a proper co-alignment of the energy levels. CNT are also expected to act as nucleating agents for the semi-crystalline conjugated polymers comprising the electron-donor moiety in POPV and thus increase the degree of crystallinity. This in turn should shift the optical absorption of the polymer to longer wavelengths ("red-shift") and improve the effective mobility of holes transported via the polymer channel.[52] We note here that CNT were also suggested as the major components in transparent conductive electrodes (as a replacement for indium tin oxide (ITO)), but this topic is beyond the scope of this article.

Nowadays, cost-effective production of CNT is enabled due to the development of ton-scale technology.[53]

Yet, the utilization of CNT as functional components in photoactive hybrids was found to difficult and challenging: The different methods used for synthesis of CNT powders which include arc discharge, laser ablation, chemical vapor deposition[41,42] result in mixtures of CNT that are structurally and electronically heterogeneous. Thus, as-produced SWCNT powders contain mixtures of conducting and semiconducting SWCNT with a distribution of diameters and lengths. In addition, amorphous carbon, graphitic and metallic particles are present in the soot, resulting in typically low purity of 30–70 vol %, as compared to fullerenes where 99.9 vol % purity characterizes the high ("golden") grade and 99.5 vol % in industrial products. Long and aggressive purification processes of SWCNT samples result in purity of 90–95 vol %.[54]

The purification processes are commonly based on acid treatment and oxidation for removal of the metallic and carbonaceous impurities. This treatment is known to alter significantly the electronic properties of SWCNT as some oxidation of the tubes sidewalls is inevitable.[55] The defects introduced by the processes act as scattering sites and reduce charge carrier mobility.

Furthermore, the as-produced tubes emerge from the reaction mostly as crystalline structures known as ropes or bundles (Fig. 6 (c)).[56] Held together by contact energy of 40,000 k_bT for 1 micron long SWCNT (Fig. 6 (d)),[57,58] these Van der Waals crystals consist of hundreds tubes. The bundled tubes are further entangled into networks which make them non-dispersible in most common solvents.

Bundling decreases the effective CNT-polymer interfacial area and therefore reduces the efficiency of the photoinduced charge transfer. In addition, as bundling reduces the effective aspect ratio of the objects, a much higher concentration is required for the formation of a conductive network of bundles (as compared with individual tubes). Furthermore, the electrical behavior of SWCNT bundles differs from that of individual tubes. Indeed, first-principle calculations for a tube embedded in a bundle reveal that the broken symmetry of a tube caused by tube-tube interactions induces a pseudo-gap of about 0.1 eV at Fermi energy and thus modifies the electrical properties of the tube.[59]

Utilization of CNT relies on the ability to de-bundle the tubes, disperse them in a solvent, and in the context of POPV, blend individual tubes with a conjugated polymer. Covalent functionalization, adsorption of surfactants and polymers were successfully used for dispersing CNT in both aqueous and organic media. A critical review presenting the advantages and drawbacks of each of the different approaches was published recently.[60] Here, we discuss briefly the covalent approach and focus on the mutual interactions between conjugated polymers and CNT.

Covalent functionalization

Covalent attachment of functional moieties such as amino, fluorine or carboxyl groups to residual acidic groups introduced during the acid-purification processes was used to disperse CNT.[60] While this approach enables preparation of CNT-based nano-composites, it is often less favorable in the context of POPV due to the modification of the π-system of the CNT. In particular, when the π bonding of the graphene layers comprising the CNT is locally altered by sigma bonds, an equivalent number of π electrons are removed from the conjugated system for each functional group, leading to severe alteration of the energy-level structure.[61] Of particular worry is the effect of covalent functionalization on the electronic properties of the potential interface for charge transfer between the nanotubes and conjugated polymers.

This is very different from the case of fullerenes where the functionalized molecules (PCBM) show improved solubility and yet preserve the electronic properties of the unmodified molecule.

Thus, an alternative approach where CNT are dispersed in organic solvents using conjugated polymers as the dispersing agents was suggested.

Conjugated polymers as dispersing agents for CNT

A non-covalent pathway for dispersion of SWCNTs in organic media relies on the use of polymers for dispersing small bundles and individual CNT in organic solvents (Fig. 7).[62–65] The process is assisted by mild sonication that leads to momentary dispersion of the tubes in a solution. The co-dissolved polymers adsorb onto the CNTs and present a steric barrier that prevents re-aggregation of the CNT.

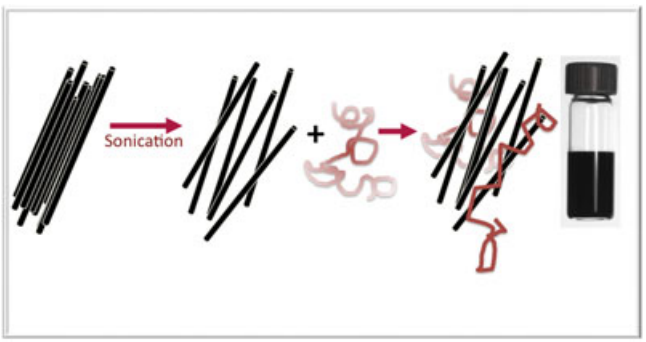

Figure 7. Sonication assisted dispersion of pristine SWCNT powder in a polymeric solution.[58,65] This figure is available in colour online at wileyonlinelibrary.com/journal/pat.

While this approach is generic and applies to a variety of polymers, here we focus on conjugated polymers. Survey of the literature reveals adsorption of conjugated polymers may result in either "wrapping"[64] or "stacking"[66] of the conjugated polymer onto the CNT (Fig. 8 (a), (b), (c)).

In the first model, the molecular geometry of the association of the conjugated polymer with the tube is helical (or double helical) wrapping of the tubes by the polymers. Wrapping of CNTs by a polymer may be driven by chemical interactions between the π-system of the CNT and the functional groups comprising the polymer or electrostatic interactions in polar media. It is now well accepted that polymer-wrapped CNTs are strongly associated, tightly bound systems (Fig. 8 (a,b)) where the tube surface chemistry, electronic structure and the intrinsic inter-tube interactions are modified by the wrapping.[67]

In the second type of interaction, part of the polymer chains adsorb via $\pi-\pi$ interactions on top of the tubes, while additional chains stack upon the chains (Fig. 8 (c)).[66] Studies of the electronic structure of the formed hybrids suggest that they exhibit distinct electronic structure[67] as well as charge transfer at the ground state.

Whether a conjugated polymer wraps or stacks onto a CNT depends on the stiffness of the polymer and the chirality and diameter of the tubes. A semi-flexible polymer such as poly (*m*-phenylenevinylene-*co*-2,5-dioctylvvoxy*p*-phenylenevinylene) was found to wrap around SWNTs.[67] Functional conjugated polymers such as poly(p-phenyleneethynylene) (PPE) that are characterized by a rigid backbone were found to stack on the nanotube surface via π-stacking without wrapping.[68,69]

P3ATs represents an intermediate case, where the persistence length of a polymer is sensitive (among other properties of the polymer) to the length of the side chains and the regioregulairty. In good solvents for P3HT, a persistence length below 3 nm was measured[70] suggesting that P3HT acts as a semi-flexible polymer in dilute solutions.[71] Yet, planarization of the polymer backbone is observed in the solid state and in the aggregated state in poor solvents.[72] One may conclude that in the case of P3HT, the configuration should depend on the detailed structure of the CNT and the processing conditions.

The detailed adsorption mechanism of P3HT chains on the surface of CNT was discussed by Boon *et al.*[66] In a study

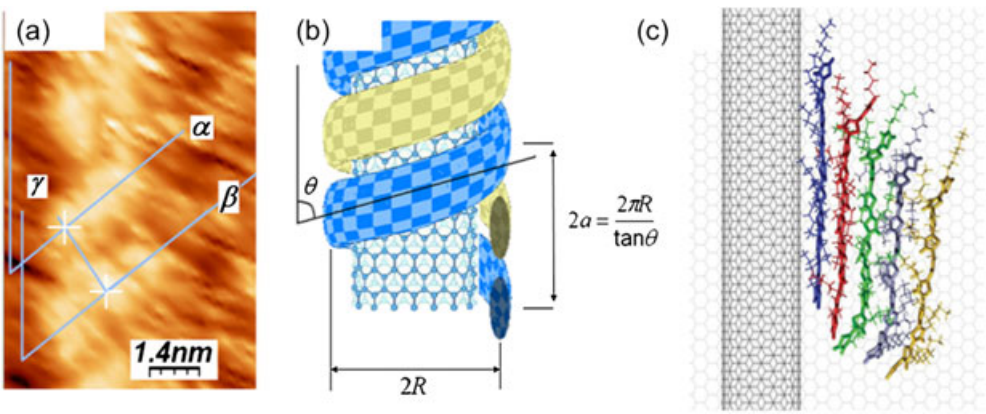

Figure 8. Scanning tunneling microscopy image (a) and a schematic representation (b) of a MWCNT covered by rr-P3HT self-organized into a coiled structure, Reprinted with permission from ref.[64] Copyright 2012, American Institute of Physics. (c) Snapshot extracted from MD simulation of short P3HT assembly on top the SWNT following ref.[66] This figure is available in colour online at wileyonlinelibrary.com/journal/pat

combining experiments study and computer simulations, they showed that due to $\pi-\pi$ interactions between thiophene units and the $\pi-$ system of MWNT as well as CH $-\pi$ interactions with the hexyl side chains, the polymer adopts a flat configuration on the MWNT. The initial adsorption of individual chains from solution was followed by gradual growth of P3HT fibrils by π-stacking of additional chains (Fig. 8 (c)).

It was shown that tri-block copolymers that contain a middle block comprising a conjugated polymer and two non-conjugated tails (for example ref.[73]) may be used for dispersing small bundles and individual tubes without strongly affecting the electronic and optical properties of the tube. Here, the middle block was too short to wrap around the CNT and the solvated, non-adsorbing tails induced weak (on the order of a few k_BT) steric repulsion[74] at a large inter-tube distance (few to tens of nanometers). At this inter-tube separation, the attractive interaction between adjacent tubes is much smaller than k_BT (see Fig. 6 (d)), and thus the weak-long ranged repulsion prevents aggregation of the individually dispersed tubes.[73,74]

CNT doping

The electronic properties of CNT may be tailored by the presence of minute (from parts per million) concentrations of atoms and molecules that act as electron donors or electron acceptors with respect to the conjugated π-system comprising the tubes. Doping often occurs unintentionally as in the case of exposure of CNT to ambient conditions where oxygen molecules adsorb to the CNT and lead to p-type behavior of "pristine" CNT.

Intentional doping may be carried out in conditions that result in exohedral doping (or intercalation), endohedral doping (or encapsulation) and in-plane or substitutional doping. The full topic of CNT doping is beyond the scope of this article. For a comprehensive review, see for example ref.[75]

Chemical doping is expected to substantially enhance the electrical conductivity of CNT. PCE of 4.1% was reported in BHJ devices based on fullerene-polymer active layer that contained 1 wt% of well-dispersed boron-doped MWCNT.[11] Following a methodical study of the performance of solar cells based on nitrogen-doped (n-doped) and boron-doped (p-doped) MWCNT, the authors suggested that the origin of the improved performance is an improved hole transport via the doped CNT network leading to an overall better balance of electron and hole transport throughout the device.

The early attempts to utilize CNT in polymer-based solar cells were motivated by the hope that they may replace fullerenes in BHJ solar cell and serve simultaneously to improve the crucial functions of charge separation, charge collection and charge transport. In reality, it was found that the actual functionality of the CNT in the device varied and depended on the type of the CNT the processing conditions and the interfacial interactions at the conjugated polymer-CNT interface.

CNT-BASED PPV

The early years 1999–2008

Early studies, from about 10 years ago, of CNT-conjugated polymers reported very low efficiency of CNT-based solar cells.[76]

The first report of a device utilizing CNTs (MWCNT) as a component in POPV was published in 1999 by Ago *et al.*[9] Untreated MWCNT were used to prepare a p-phenylene vinylene (PPV)- MWCNT bi-layer where the MWCNT was intended to serve as a hole-collecting electrode. Yet, the results indicated that the processes did not involve electron transfer, and in a later study using photoinduced absorption spectroscopy,[77] the authors discovered that energy transfer (rather than electron transfer) took place between the PPV and MWCNT layers.

In 2002, the idea of using SWCNTs as acceptors in BHJ solar cells was proposed by Kymakis *et al.*[78] Enhancement of more than two orders of magnitude in the photocurrent, as compared to single component P3OT cells, was observed due to the addition of about 1 wt% SWCNT. While the authors speculated that the SWCNT improved charge separation, the power conversation efficiency was 0.04% under 100 mW/cm^2 illumination, well below that for typical BHJ POPV cells. The authors suggested that a poor dispersion of the SCWNT and the presence of a mixture of metallic and semiconducting tubes were the reasons for the low efficiency. The same group demonstrated some years later[79] that the annealing of an active layer which contains P3HT-SCWNT blend results in an increase in cell efficiency compared to un-annealed cells. Here, the improved efficiency may be related to improved hole transport via the polymer matrix due to a higher degree of crystallinity induced by the presence of the SWCNT. This indirect effect of the CNT on the assembly of the polymer matrix demonstrates once again the complexity of the system.

Kazoui *et al.*[80] were the first to consider the effect of the purification process on the CNT structure. To void disruption of the tube, they dispersed the CNT via a conjugated polymer and did not use acid treatment. They described the behavior of the different types of tubes and stressed that while s-SWCNTs act as light harvesting centers in donor polymer matrices, matching the solar spectrum with 0.8 nm diameter tubes, both semiconducting SWCNTs and metallic SWCNTs were expected to contribute to charge separation, collection and transport.

Rodolfo, *et al.*[81] suggested that SWCNT may be used for increasing the V_{oc}. In most OPV, especially devices containing CNT, the V_{oc} is typically below 1 V. The proposed strategy relied on the insertion of a continuous polymer layer between the electrode and the layer containing the SWCNTs so as to hinder the short cuts and shunts caused by metallic SWCNT. Indeed, V_{oc} of 1.2 V was measured in those devices demonstrating that high concentrations of SWCNTs may be used without short circuiting the device.

The early attempts to utilize CNT as active components in POPV resulted in devices of low-power conversion efficiencies as compared to that measured in PCBM-based POPV, mainly due to low values of the photocurrent. Analysis of the studies indicates that uncontrolled interactions at the CNT-polymer interface not only reduced the effectiveness of the tubes as charge transporters but also interfered with the photo-physical processes by acting as recombination centers for excitions (metallic SWCNT) or as energy quenchers (P3HT- s- SWCNT), and by shortcutting the electric circuit (long CNT). The most important insight emerging from these studies is the realization of the importance of interfacial interactions and the need for rational design of the CNT-polymer interface all the way from the nano to the meso scale.

Recent studies 2008–2011

It is now evident that control over the structure and properties of the conjugated polymer-CNT blend, at length scales ranging

from the molecular to the sub-micron range, is one of the most difficult as well as crucial issues for efficient photocurrent collection in CNT-based OPV devices. Furthermore, as aggressive surface treatment was found to alter the electronic properties of the CNT, an effort is being made over the last few years to develop processing methods for CNT that would take into account the structural integrity of the CNT, the complex polymer-solvent-CNT interactions, and the effect of CNT on the conjugated polymer matrix.

For example, in a recent study, Chang *et al*.[82] showed that the performance of CNT-P3HT POPV was correlated to the quality of the CNT dispersion in P3HT solutions and dominated by interaction of the CNT and the polymer with the solvent. This observation is not surprising, as it is well established that in fullerene–polymers solar cells, the morphology and performance of the device strongly depend on the interactions of both the conjugated polymer and the fullerenes with the solvent.

Arranz-Andres and Blau[83] studied the influence of the CNT dimensions (length and diameter) and their concentration in the POPV photoactive layer on the performance of a CNT-polymer device. They found that 5 wt% of CNT increased PCE by three orders of magnitude compared to that of the native polymer. The study reported that the introduction of CNTs into the P3HT matrix modified the energy levels of the P3HT (as evidenced by high V_{oc}) and the morphology of the active layer. They also found that the CNT acted as nucleation sites for P3HT chains, improved charge separation (as indicated by the large difference between light and dark conductivities) and served as networks for electron transport.

Evidence for correlations between the interactions at the conjugated polymers-CNT interface and the performance of the blend was found in a few studies. Furthermore, it was shown that these interactions are more important than the electronic structure of the pristine polymer (or the tubes).

For example, Singha *et al*. and Mallajosyula *et al*.[84,85] carried out a comprehensive study in which it was found that POPV based on SWCNT-P3OT showed higher efficiencies as compared to SWCNT-P3HT devices. This behavior cannot be attributed to the difference between the HOMO–LUMO gap of the polymers since these are only 0.05 eV apart. In addition, it was reported that similar photocurrent values were measured in poly(phenyleneethynylene) PPE-SWCNT system[86] and P3OT-SWCNT-based devices, with a higher V_{oc} value in the P3OT system. The PCE values were 0.05% in the SWCNT-PPE device and 0.02% in the SWCNT-P3OT system. This observation is rather striking as the HOMO–LUMO gap of P3HT is 2 eV while that of PPE is 2.4 eV, thus photoexcitation should be more favorable in P3HT even if electron transfer is considered. The authors suggested that a better dispersion of the SWCNTs in PPE could be the origin of the higher efficiency.

Three component systems

The difficulties in utilization of CNT as electron acceptors with yet the need to replace fullerenes by more efficient and geometrically more favorable moieties for electron transport have led to the suggestion of using CNT exclusively for charge transport in a three-component CNT-fullerene-conjugated polymer system. It was suggested that by combining both low concentrations of PCBM and CNT, one may be able to still utilize fullerenes (and PCBM) for efficient charge separation while CNT with their superior electron transport properties, and their low percolation threshold ($<$ 0.1 wt%) would serve for setting high-mobility pathways for electron transport.[86]

The suggested configuration is presented in Fig. 9.

The same group[87] produced novel immobilized C_{60}–SWCNT complexes. These complexes were used in the photoactive layer of a BHJ POPV cell with P3HT. The authors compared the result to a control device where the C_{60} were exclusively used as the electron acceptors and concluded that the addition of SWCNTs resulted in an improvement of both the short circuit current density (J_{sc}) and the FF.[87] Two types of MWCNT were compared with C_{60}, one carrying carboxyl group, *c*-MWCNT, and the other a long alky chain *o*-MWCNT. Both CNT types were complexed with C_{60} using microwave radiation. The measured PV performance of the resulting BHJ devices was found to be highly sensitive to the functional group with significant improvement of the cell efficiency of the P3HT:*c*-MWCNT/C_{60} device, to 0.80% compared to 0.10% for the P3HT:*o*-MWCNT/C60 cell. The differences in efficiency between the two variations were mainly attributed to the electron withdrawing nature of the carboxyl group on the *c*-MWCNT, and the electron blocking effect of the long alky chain on the *o*-MWCNT. In both of these studies, the authors analyzed the improved performance in terms of the efficiency of charge transfer between the PCBM and the CNT, but no direct evidence was provided.

Berson *et al*.[88] were among the first to describe a methodical study of the dispersion processes of CNT followed by preparation of BHJ solar cells where the active layer comprises the three-components, P3HT-PCBM-CNT. In this well-characterized system, the PCE values finally reached 2%. We note here that unpurified SWCNT may act as stronger acceptors than PCBM in the P3HT-PCBM system, but if the electron are not extracted from the SWCNT, lower efficiency will be measured as the CNT then act as electron traps, as was shown in a different system.[89]

Another study conducted by Pradhan *et al*. using 90% semiconducting nanotubes reported that the effect of exohedral fullerenes on the electronic properties CNT is essentially that of n-doping. The resulting PCBM-doped s-SWCNTs demonstrated significantly enhanced electrical conductivity, while still retaining the characteristics of semiconducting nanotubes.[90]

Bindl *et al*.[91] studied the exciton dissociation and interfacial charge transfer from semiconducting s-SWCNT, to a variety of polymeric photovoltaic materials using a photoactive capacitor measurement technique. They showed that photogenerated

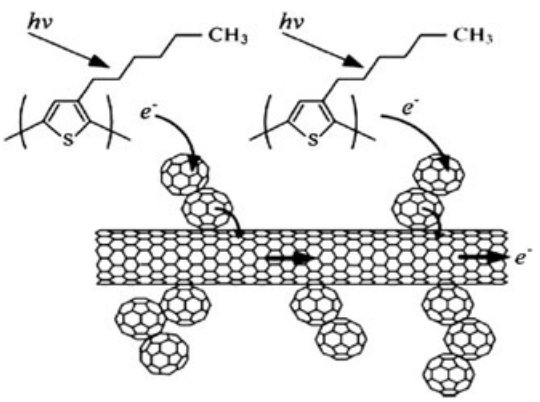

Figure 9. Light absorption by P3HT leads to photoinduced charge separation at the polymer–C_{60} interface, followed by electron transfer from C_{60} to the SWNT tubes (Reproduced by permission of the Royal Society of Chemistry).[86]

excitons on s-SWCNT in thin films are dissociated at interfaces with C_{60}, PCBM, P3OT, as well regioregular and regiorandom P3HT. Photocurrent bias dependencies revealed that fullerene and poly(thiophene) derivatives serve as electron-accepting and hole-accepting materials to s-SWCNTs, respectively.

In a recent study, Derbal *et al.*[92] demonstrated that the introduction of 0.2% of functionalized SWCNTs in P3HT–PCBM conventional solar cells improved the V_{oc} up to 0.76 eV with an efficiency of 3.8%. The incorporation of a functionalized SWCNT in this type of solar cell improves both the current density J_{sc} and the open circuit voltage V_{oc}, but not simultaneously. Interestingly, in the presence of functionalized CNT, the maximal theoretical V_{oc} as predicted by the HOMO–LUMO energy difference of the heterojunction was approached. However the underlying mechanism remains unknown.

Finally, we note that placement of CNT at the cathodic side of the active layer in a polymer-fullerene solar cells resulted in PCE of 4.9%, while their placement at the anodic side was found to result in zero-field PV devices. This is correlated with the observation that the UV–vis absorption spectra of PCBM is altered by the SWCNTs and suggests that SWCNTs interact with the active layer.[93]

The studies described so far focused on the preparation and characterization of thin-film POPV devices. Other geometries such as fiber-shaped hybrids were suggested for energy-harvesting textiles.[94,95] While control over the mesosocopic morphology of the hybrid was demonstrated actual utilization of PV-active fibers for preparation of BHJ solar cells based on an individual fiber, photovoltaic textile-based solar panels or OPV cells with conductive mesh grids is yet to be perceived.

CONCLUDING REMARKS AND FUTURE PRESPECTIVES

Conjugated polymers combine optoelectronic properties of semiconductors with mechanical properties and processing advantages of polymers. As discussed throughout this article, the optical and electronic characteristics of conjugated polymers are primarily governed by the nature of the molecular conjugation which may be designed via organic synthesis. Currently, the main efforts in the field are focused on the development of conjugated polymers with lower optical bandgap that are yet solvent-processable and reasonably stable at ambient conditions.

The new materials are then used along with electron acceptors, such as fullerenes and CNTs for preparation of functional hybrids that act as the active layer in BHJ POPV. The performance of the active layer depends not only on the structure of the different components but also on their spatial organization at the nano to meso scales. The morphology which is determined by interfacial and intermolecular interactions *between* the components may or may not promote the desired performance of the active layer.

While morphology–performance relations have been thoroughly investigated in fullerene-based hybrids, the effect of CNTs on the polymer-fullerene system is relatively unexplored. The inherent structural and morphological heterogeneity of as-produced CNT powders and the sensitivity of the polymer-CNT system to processing conditions contribute to the diversity of the reported observations and the sometimes controversial conclusions.

Furthermore, the fundamental physics of charge transfer and charge transport between conjugated polymers and CNT as well as the self-assembly and phase morphology of conjugated polymers-CNT hybrids is far from being understood. In particular, it is not yet clear which type of CNT, under which conditions, can be used as interface for excition dissociation, charge transporters (holes or electrons) or contribute indirectly to the self-organization of the conjugated polymer layer.

We believe that the large progress that has been made over the last decade in regulating the structure and properties of CNT will enable researchers to design and carry out well-controlled experiments that will lead to a significant progress in the understanding of the fundamentals of the optoelectronic behavior of polymer-CNT hybrids. In parallel, the establishment of particular processing pathways each adequate for a different end-product and the progress in characterization of the resulting hybrids is expected to improve the properties and the consequential performance of CNT-based POPV.

The future of conjugated polymers–CNT hybrids as active materials in POPV will depend on the rate of progress in the two parallel routes of fundamental research and design of technologically feasible routes for structural engineering at the nano to the meso scale of CNT-conjugated polymers hybrids.

Acknowledgements

R.Y-R holds the Stanley D. and Nikki Waxberg professorial chair in Advanced Materials. R.Y-R and E.K thanks the Focal Initiatives in Science and Technology Foundation of the Israel Science Foundation, Grant No. 1004/07, and R. Y-R thanks as well the Israel Science Foundation grant no. 208/09.

REFERENCES

[1] B. Minnaert, M. Burgelman, *Prog. Photovolt. Res. Appl.* **2007**, *15*, 741–748.
[2] S. E. Shaheen, R. Radspinner, N. Peyghambarian, G. E. Jabbour, *Appl. Phys. Lett.* **2001**, *79*, 2996–2998.
[3] B. Winther-Jensen, F. C. Krebs, *Sol. Energ. Mater. Sol. Cell* **2006**, *90*, 123–132.
[4] M. A. Green, K. Emery, Y. Hishikawa, W. Warta, E. D. Dunlop, *Prog. Photovolt. Res. Appl.* **2011**, *19*, 565–572.
[5] M. A. Green, K. Emery, Y. Hishikawa, W. Warta, E. D. Dunlop, *Prog. Photovolt. Res. Appl.* **2012**, *20*, 12–20.
[6] M. Jørgensen, K. Norrman, S. A. Gevorgyan, T. Tromholt, B. Andreasen, F. C. Krebs, *Adv. Mater.* **2011**, *24*, 580–612.
[7] N. S. Sariciftci, L. Smilowitz, A. J. Heeger, F. Wudl, *Science* **1992**, *258*, 1474–1476.
[8] S. Morita, A. A. Zakhidov, K. Yoshino, *Sol. State Commun.* **1992**, *82*, 249–252.
[9] H. Ago, K. Petritsch, M. S. P. Shaffer, A. H. Windle, R. H. Friend, *Adv. Mater.* **1999**, *11*, 1281–1285.
[10] E. Kymakis, G. Amaratunga, *APL* **2002**, *80*, 112.
[11] J. Min Lee, J. S. Park, S. H. Lee, H. Kim, S. Yoo, S. Ouk Kim, *Adv. Mater.* **2011**, *23*, 629–633.
[12] C. K. Chiang, C. R. Fincher, Jr., Y. W. Park, A. J. Heeger, H. Shirakawa, E. J. Louis, S. C. Gau, A. G. MacDiarmid, *Phys. Rev. Lett.* **1977**, *39*, 1098–1101.
[13] M. P. Swenberg, *Electronic Processes in Organic Crystals and Polymers*. Oxford press, London, **1999**.
[14] C. J. Brabec, V. Dyakonov, U. Scherf, *Organic photovoltaics: materials, device physics, and manufacturing technologies*. Wiley-VCH, Weinheim, **2008**.
[15] A. Kraft, A. C. Grimsdale, A. B. Holmes, *Ang. Chem. Int. Ed.* **1998**, *37*, 402–408.
[16] R. D. McCullough, R. D. Lowe, M. Jayaraman, D. L. Anderson, *J. Org. Chem.* **1993**, *58*, 904–912.
[17] R. D. Reike, *J. Am. Chem. Soc.* **1995**, *117*, 233–244.

[18] V. Causin, C. Marega, A. Marigo, L. Valentini, J. M. Kenny, *Macromolecules* **2005**, *38*, 409–415.
[19] F. Jonas, L. Schrader, *Synth. Met.* **1991**, *41–43*, 831–836.
[20] J. Ouyang, Q. Xu, C.-W. Chu, Y. Yang, G. Li, J. Shinar, *Polymer* **2004**, *45*, 8443–8450.
[21] M. K. Siddiki, J. Li, D. Galipeau, Q. Qiao, *Energ. Environ. Sci.* **2010**, *3*, 867–883.
[22] C. Winder, N. S. Sariciftci, *J. Mater. Chem.* **2004**, *14*, 1077–1086.
[23] M. Kobayashi, N. Colaneri, M. Boysel, F. Wudl, A. J. Heeger, *J. Chem. Phys.* **1985**, *82*, 5717–5723.
[24] M. Helgesen, S. A. Gevorgyan, F. C. Krebs, R. A. J. Janssen, *Chem. Mater.* **2009**, *21*, 4669–4675.
[25] A. Dhanabalan, J. K. J. van Duren, P. A. Van Hal, J. L. J. van Dongen, R. A. J. Janssen, *Adv. Funct. Mater.* **2001**, *11*, 255–262.
[26] A. Dhanabalan, P. A. van Hal, J. K. J. van Duren, R. A. J. Janssen, *Synth. Met.* **2001**, *121*, 2175–2180.
[27] J. Peet, J. Y. Kim, N. E. Coates, W. A. Ma, D. Moses, A. J. Heeger, G. C. Bazan, *Nat. Mater.* **2007**, *7*, 497–500.
[28] P. Zoombelt, S. G. J. Mathijssen, M. G. R. Turbiez, M. M. Wienka, R. A. J. Janssen, *J. Mater. Chem.* **2010**, *20*, 2240–2246.
[29] Nobel lecture, A. J. Heeger, http://www.nobelprize.org/nobel_prizes/chemistry/laureates/2000/heeger-lecture.html
[30] F. Perepichka, D. F. Perepichka, *Handbook of thiophene-based materials: applications in organic electronics and photonics* (vol. *2*). John Wiley and Sons, Hoboken, **2009**, 630.
[31] H. W. Kroto, J. R. Heath, S. C. O'Brien, R. F. Curl, R. E. Smalley, *Nature* **1985**, *318*, 162–163.
[32] R. C. Haddon, L. E. Brus, K. Raghavachari, *Chem. Phys. Lett.* **1986**, *125*, 459–464.
[33] R. C. Haddon, *Acc. Chem. Res.* **1992**, *25*, 127–133.
[34] R. D. Johnson, D. S. Bethune, C. S. Yannoni, *Acc. Chem. Res.* **1992**, *25*, 169.
[35] In conjugated polymers like PPV and its derivatives energy band-gap values ranging from very small (0.04 eV), C. H. Lee, G. Yu, D. Moses, A. J. Heeger, *Phys. Rev. B* **1994**, *49*, 2396–2407 to intermediate (around 0.4 eV), P.a.C. Gomes da Costa, Phys. Rev. B **1993**, *48*, 1993–1996 to very high (up to 0.95 eV), M.a.M. S Chandross, S. Jeglinski, X. Wei, Z. V. Vardeny, E. W. Kwock, T. M. Miller, *Phys. Rev. B* **1994**, *50*, 14702–14705.
[36] S. R. Scully, M. D. McGehee, *J. Appl. Phys.* **2006**, *100*, 034907–034909.
[37] E. Geckeler, S. Samal, *Polymer Int.* **1999**, *48*, 74–78.
[38] S. Günes, H. Neugebauer, N. S. Sariciftci, *Chem. Rev.* **2007**, *107*, 1324–1338.
[39] H. Peimo, X. Yabo, Z. Xuejia, Z. Xinbin, L. Wenzhou, *J. Phys. Condens. Matter.* **1993**, *5*, 7013–7016.
[40] J. K. J. van Duren, X. Yang, J. Loos, C. W. T. Bulle-Lieuwma, A. B. Sieval, J. C. Hummelen, R. A. J. Janssen, *Adv. Funct. Mater.* **2004**, *14*, 425–434.
[41] M. S. Dresselhaus, G. Dresselhaus, P. Avouris, *Carbon Nanotubes, Topics in Applied Physics 80*, Springer–Verlag, Berlin Heidelberg, **2001**.
[42] S. Cataldo, P. Salice, E. Menna B. Pignataro, *Energ. Environ. Sci.* **2012**, *5*, 5919–5940.
[43] V. I. Arkhipov, H. Bässler, *Phys. Stat. sol. (a)* **2004**, *201*, 1152–1187.
[44] N. Kazaoui, B. Minami, Y. Nalini, K. Kim, K. Hara, *J. Appl. Phys.* **2005**, *98*, 084314–084316.
[45] J. Arranz-Andrés, W. J. Blau, *Carbon* **2008**, *46*, 2067–2075.
[46] C. Yang, M. Wohlgenannt, Z. V. Vardeny, W. J. Blau, A. B. Dalton, R. Baughman, A. A. Zakhidov, *Phys. B Condens. Matter.* **2003**, *338*, 366–369.
[47] J. Luo, L.-M. Peng, Z. Q. Xue, J. L. Wua, *J. Chem. Phys.* **2004**, *120*, 7998–8001.
[48] J. H. Shim, T. Back, K. W. Kwon, *Phys. Rev. B* **2005**, *71*, 205411.
[49] J. Ferguson, J. F. Andrew, J. L. Blackburn, J. M. Holt, N. Kopidakis, R. C. Tenent, T. M. Barnes, M. J. Heben, G. Rumbles, *J. Phys. Chem. Lett.* **2010**, *1*, 2406–2411.
[50] V. Dyakonov, G. Zoriniants, M. Scharber, C. J. Brabec, R. A. J. Janssen, J. C. Hummelen, N. S. Sariciftci, *Phys. Rev. B* **1999**, *59*, 8019–8025.
[51] A. Konkin, C. Bounioux, U. Ritter, P. Scharff, E. A. Katz, A. Aganov, G. Gobsch, H. Hoppe, G. Ecke, H.-K. Roth, *Synth. Met.*, **2011**, *161*, 2241–1148.
[52] K. P. Ryan, S. M. Lipson, A. Drury, M. Cadek, M. Ruether, S. M. O'Flaherty, V. Barron, B. McCarthy, H. J. Byrne, W. J. Blau, *et al. Phys. Lett.* **2004**, *391*, 329–333.
[53] The nanotube site http://www.pa.msu.edu/cmp/csc/nanotube.html and H. G. Tennent, J. J. Barber, R. Hoch, US Patent 5, 578,543, **1996**.
[54] M. Monthioux, B. W. Smith, B. Burteaux, A. Claye, J. E. Fischer, D. E. Luzzi, *Carbon* **2001**, *39*, 1251–1272.
[55] P.-C. Ma, N. A. Siddiqui, G. Marom, J.-K. Kim, *Composites Part A* **2010**, *41*, 1345–1367.
[56] A. Thess, R. Lee, P. Nikolaev, H. Dai, P. Petit, J. Robert, C. Xu, Y. H. Lee, S. G. Kim, A. G. Rinzler, D. T. Colbert, G. E. Scuseria, D. Tománek, J. E. Fischer, R. E. Smalley, *Science* **1996**, *273*, 483–487.
[57] L. A. Girifalco, M. Hodak, R. S. Lee, *Phys. Rev. B* **2000**, *62*, 13104–13110.
[58] R. Shvartzman- Cohen, E. Nativ-Roth, E. Baskaran, Y. Levi- Kalisman, I. Szleifer, R. Yerushalmi-Rozen, *J. Am. Chem. Soc.* **2004**, *126*, 14850–14857.
[59] P. Delaney, H. J. Choi, J. Ihm, M. L. Cohen, *Nature* **1998**, *391*, 466–468.
[60] B. R. Suryasarathi, A. Khare, P. Moldenaers, *Polymer* **2010**, *51*, 975–993.
[61] H. Hu, B. Zhao, M. A. Hamon, K. Kamaras, M. E. Itkis, R. C. Haddon, *J. Am. Chem. Soc.* **2003**, *125*, 14893–14900.
[62] B. Z. Tang, H. Xu, *Macromolecules* **1999**, *32*, 2569–2576.
[63] A. B. Dalton, W. J. Blau, G. Chambers, J. N. Coleman, K. Henderson, S. Lefrant, B. McCarthy, C. Stephan, H. J. Byrne, *Synth. Met.* **2001**, *121*, 1217–1218.
[64] M. Giulianini, E. R. Waclawik, J. M. Bell, M. De Crescenzi, P. Castrucci, M. Scarselli, N. Motta, *AIP* **2009**, *95*, 013304.
[65] I. Szleifer, R. Yerushalmi-Rozen, *Polymer* **2005**, *46*, 7803.
[66] F. Boon, S. Desbief, L. Cutaia, O. Douhéret, A. Minoia, B. Ruelle, S. Clément, O. Coulembier, J. Cornil, P. Dubois, *et al*., *Macromol. Rapid Comm.* **2010**, *31*, 142–144.
[67] B. McCarthy, J. N. Coleman, R. Czerw, A. B. Dalton, M. in het Panhuis, A. Maiti, A. Drury, P. Bernier, J. B. Nagy, B. Lahr, H. J. Byrne, D. L. Carroll, W. J. Blau, *Phys. Chem. B* **2002**, *106*, 2210–2015.
[68] J. Chen, H. Liu, W. A. Weimer, M. D. Halls, D. H. Waldeck, G. C. Walker, *J. Am. Chem. Soc.* **2002**, *124*, 9034.
[69] J. Zhao, J. P. Lu, J. Han, C. K. Yang, *Appl. Phys. Lett.* **2003**, *82*, 3746.
[70] G. W. Heffner, D. S. Pearson, *Macromolecules* **1991**, *24*, 6295.
[71] T. Yamamoto, D. Komarudin, M. Arai, B. Lee, H. Suganuma, N. Asakawa, Y. Inoue, K. Kubota, S. Sasaki, T. Fukuda, *et al. J. Am. Chem. Soc.* **1998**, *120*, 2047.
[72] P. V. Shibaev, K. Schaumburg, T. Bjornholm, K. Norgaard, *Synth. Met.* **1998**, *97*, 97–104.
[73] R. Itzhak, D. Raichman, Z. Shahar, G. L. Frey, J. Frey, R. Yerushalmi–Rozen, *J. Phys. Chem. C* **2010**, *114*, 3748–3753.
[74] E. Nativ-Roth, R. Shvartzman-Cohen, C. Bounioux, M. Florent, D. Zhang, I. Szleifer, R. Yerushalmi-Rozen, *Macromolecules* **2007**, *40*, 3676–3685.
[75] L. Duclaux, *Carbon* **2002**, *40*, 1751–1764.
[76] M. Baibara, P. Gómez-Romero, *J. Nanosci. Nanotechnol.* **2006**, *6*, 1–14.
[77] H. Ago, *Phys. Rev. B* **2000**, *61*, 2286.
[78] E. Kymakis, G. A. J. Amaratunga, *Appl. Phys. Lett.* **2002**, *80*, 112–114.
[79] E. Kymakis, E. Koudoumas, I. Franghiadakis, G. A. J. Amaratunga, *J. Phys. D: Appl. Phys.* **2006**, *39*, 1058–1062.
[80] S. Kazaoui, N. Minami, B. Nalini, Y. Kim, K. Hara *J. Appl. Phys.* **2005**, *98*, 084314.
[81] L. Rodolfo, B. S. L. Patyk, A. F. Nogueira, C. A. Furtado, A. P. Santos, R. M. Q. Mello, L. Micaroni, I. A. Hümmelgen, *Phys. Status Solidi Rapid Res. Lett.* **2007**, *1*, R43-R45.
[82] C. K. Chang, J. Y. Hwang, W. J. Lai, C. W. Chen, C. I. Huang, K. H. Chen, L. C. Chen, *Chem. J. Phys.* **2010**, *C114*, 10932–10936.
[83] J. Arranz-Andres, W. Blau, *Carbon* **2008**, *46*, 2067–2075.
[84] I. Singh, P. K. Bhatnagar, P. C. Mathur, I. Kaur, L. M. Bharadwaj, R. Pandey, *Carbon* **2008**, *46*(8), 1141–1144.
[85] A. T. Mallajosyula, S. S. K. Lyer, B. Mazhari, *Jpn. J. Appl. Phys.* **2009**, *48*, 011503.
[86] C. Li Y. Chen, Y. Wang, Z. Iqbal, M. Chhowalla, S. Mitra, *J. Mater. Chem.* **2007**, *17*, 2406–2411.
[87] C. Li, Y. Chen, S. Addo Ntim, S. Mitra, *Appl. Phys. Lett.*, **2010**, *96*, 143303.
[88] S. Berson, R. de Bettignies, S. Bailly, S. Guillerez, B. Jousselme, *Adv. Funct. Mater.* **2007**, *17*, 3363–3370.
[89] M. M. Mandoc, F. B. Kooistra, J. C. Hummelen, B. de Boer, P. W. M. Blom, *Appl. Phys. Lett.* **2007**, *91*, 263505.
[90] B. Pradhan, R. R. Kohlmeyer, K. Setyowati, J. Chen, *Appl. Phys. Lett.* **2008**, *93*, 223102–3.
[91] D. J. Bindl, N. S. Safron, M. S. Arnold, *ACS Nano*, **2010**, *4*, 5657–5664.
[92] H. Derbal-Habak, C. Bergeret, J. Cousseau, J. M. Nunzi, *Sol. Energy Mater. Sol. Cells* **2011**, *95* 53–6.
[93] S. Chaudhary, H. Lu, A. M. Muller, C. J. Bardeen, M. Ozkan, *Nano Lett* **2007**, *7*, 1973–1979.
[94] C. Bounioux, R. Itzhak, R. Avrahami, E. Zussman, J. Frey, E. A. Katz, R. Yerushalmi-Rozen, *J. Polym. Sci. B* **2011**, *49*, 1263–1268.
[95] I. Shames, C. Bounioux, E. A. Katz, R. Yerushalmi-Rozen, E. Zussman, *Appl. Phys. Lett.* **2012**, *100*, 113303.